Copper(II) L/D-valine-(1,10-phen) Complexes Target Telomeric G-quadruplex Motifs and Promote Site-Specific DNA Cleavage and Cellular Cytotoxicity

Farukh Arjmand,[a,*] Surbhi Sharma,[a] Sabiha Parveen,[a] Loic Toupet,[b] Zhen Yu,[c] and J. A. Cowan[c]

[a] Department of Chemistry, Aligarh Muslim University, Aligarh 202002, India.

[b] Institut de Physique de sRennes, UMR 625, Université de Rennes 1, Campus de Beaulieu Bat. 11 A, 263 av. Général Leclerc, 35042 Rennes Cedex, France.

[c] Department of Chemistry and Biochemistry, The Ohio State University 100 West 18th Avenue, Columbus, OH 43210 (USA).

* Corresponding Author: Farukh Arjmand, E-mail**:** farukh.arjmand18@gmail.com Tel:+91 5712703893.

Table S1. Selected bond lengths for complex **1a.**

Bond lengths	**(Å)**
Cu(1)-N(1)	2.010
Cu(1)-N(3)	1.989
Cu(1)-N(2)	2.019
Cu(1)-N(1)	2.010
Cu(1)-O(1)	1.930
Cu(1)-O(1W)	2.246

Table S2. Selected bond angles for complex **1a.**

Bond Angle	**[deg]**
N(2)-Cu(1)-N(1)	81.79
N(3)-Cu(1)-O(1)	84.01
N(3)-Cu(1)-N(2)	99.08
O(1)-Cu(1)-N(1)	92.77
N(1)-Cu(1)-O(1W)	96.63

Table S3. Selected bond lengths for complex **1b.**

Bond lengths	**(Å)**
Cu(1)-O(1A)	1.937(3)
Cu(1)-N(3A)	1.979(4)
Cu(1)-N(1A)	1.995(4)

Cu(1)-N(2A)	2.018(4)
Cu(1)-O(3A)	2.307(5)
O(3A)-N(4A)	1.253(6)
O(4A)-N(4A)	1.249(7)
O(5A)-N(4A)	1.244(7)
Cu(2)-O(1B)	1.936(3)
Cu(2)-N(3B)	1.984(4)
Cu(2)-N(1B)	2.006(4)
Cu(2)-N(2B)	2.020(4)
Cu(2)-O(3B)	2.304(4)
O(3B)-N(4B)	1.252(6)
O(4B)-N(4B)	1.247(7)
O(5B)-N(4B)	1.243(6)

Table S4. Selected bond angles for complex **1b.**

Bond Angle	**[deg]**
O(1A)-Cu(1)-N(3A)	84.59(17)
O(1A)-Cu(1)-N(1A)	92.57(16)
N(3A)-Cu(1)-N(1A)	173.5(2)
O(1A)-Cu(1)-N(2A)	165.44(19)
N(3A)-Cu(1)-N(2A)	98.75(17)
N(1A)-Cu(1)-N(2A)	82.57(17)
O(1A)-Cu(1)-O(3A)	95.33(18)
N(3A)-Cu(1)-O(3A)	99.13(18)
N(1A)-Cu(1)-O(3A)	86.99(17)
N(2A)-Cu(1)-O(3A)	98.11(17)
O(1B)-Cu(2)-N(3B)	84.13(15)
O(1B)-Cu(2)-N(1B)	92.76(16)
N(3B)-Cu(2)-N(1B)	175.63(19)
O(1B)-Cu(2)-N(2B)	165.54(19)
N(3B)-Cu(2)-N(2B)	100.03(16)
N(1B)-Cu(2)-N(2B)	82.25(17)
O(1B)-Cu(2)-O(3B)	94.14(19)
N(3B)-Cu(2)-O(3B)	97.09(16)
N(1B)-Cu(2)-O(3B)	86.18(16)
N(2B)-Cu(2)-O(3B)	99.03(17)

Table S5. Non-covalent interaction of complex 1b with ct-DNA.

Name	**Distance (Å)**	**Category**	**Type**
Complex **1b**:N4A - B:DA17:OP1	4.61	Electrostatic	Attractive Charge
Complex **1b**:H11 - A:DC11:O2	2.62	Hydrogen Bond	Carbon Hydrogen Bond
A:DG12:OP1 - Complex **1b**	4.11	Electrostatic	Pi-Anion
B:DG14 - Complex **1b**:C16	5.28	Hydrophobic	Pi-Alkyl

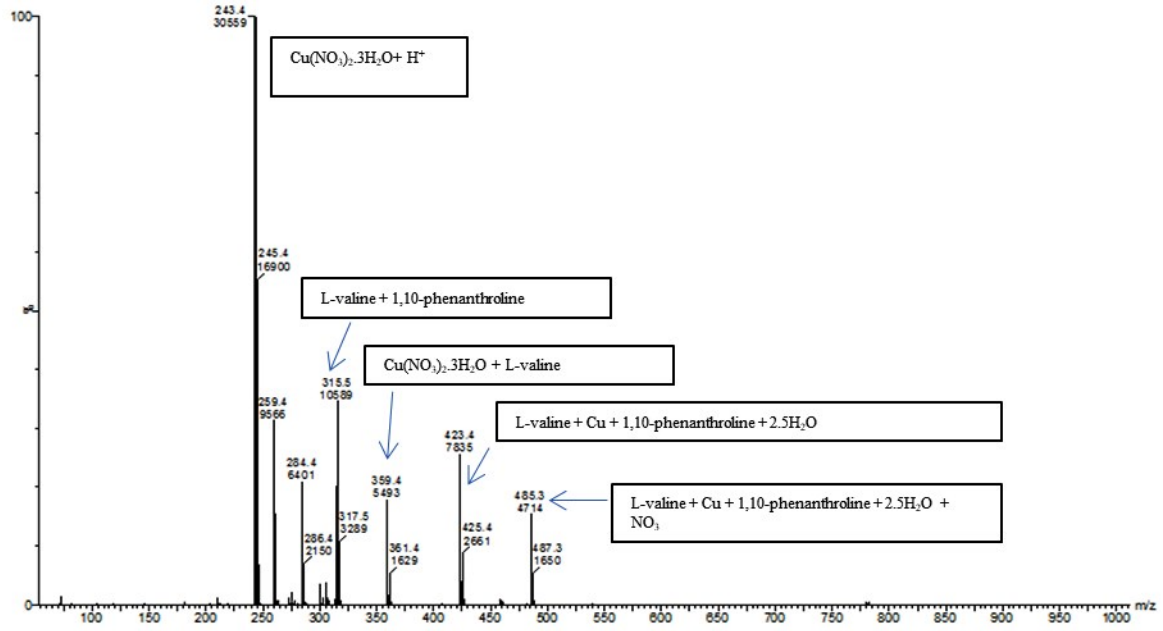

Fig. S1 ESI-MS spectrum of complex **1a.**

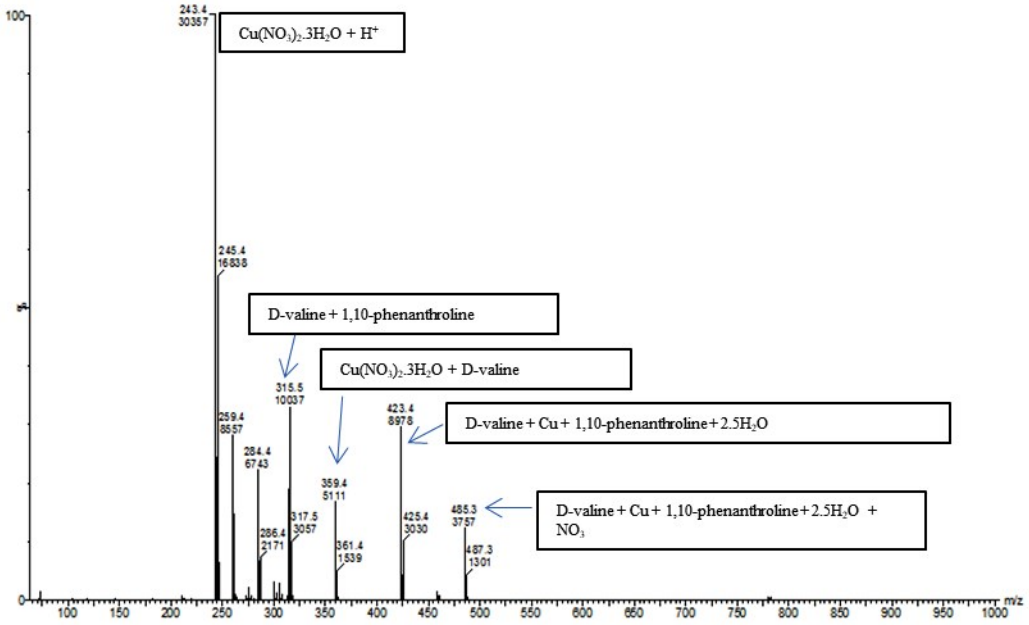

Fig. S2 ESI-MS spectrum of complex **1b.**

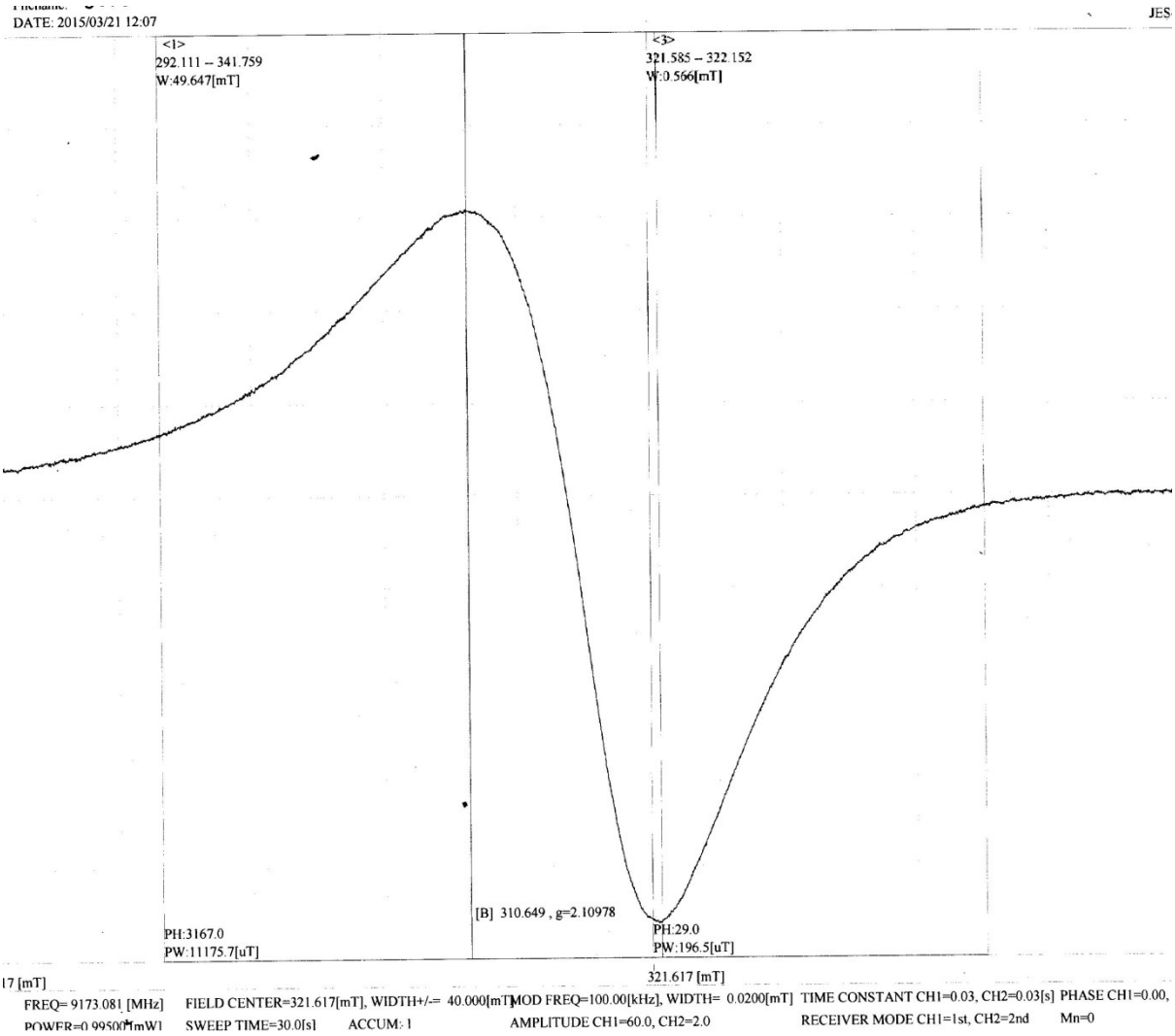

Fig. S3(i) X–band EPR spectrum of complex **1a** at RT.

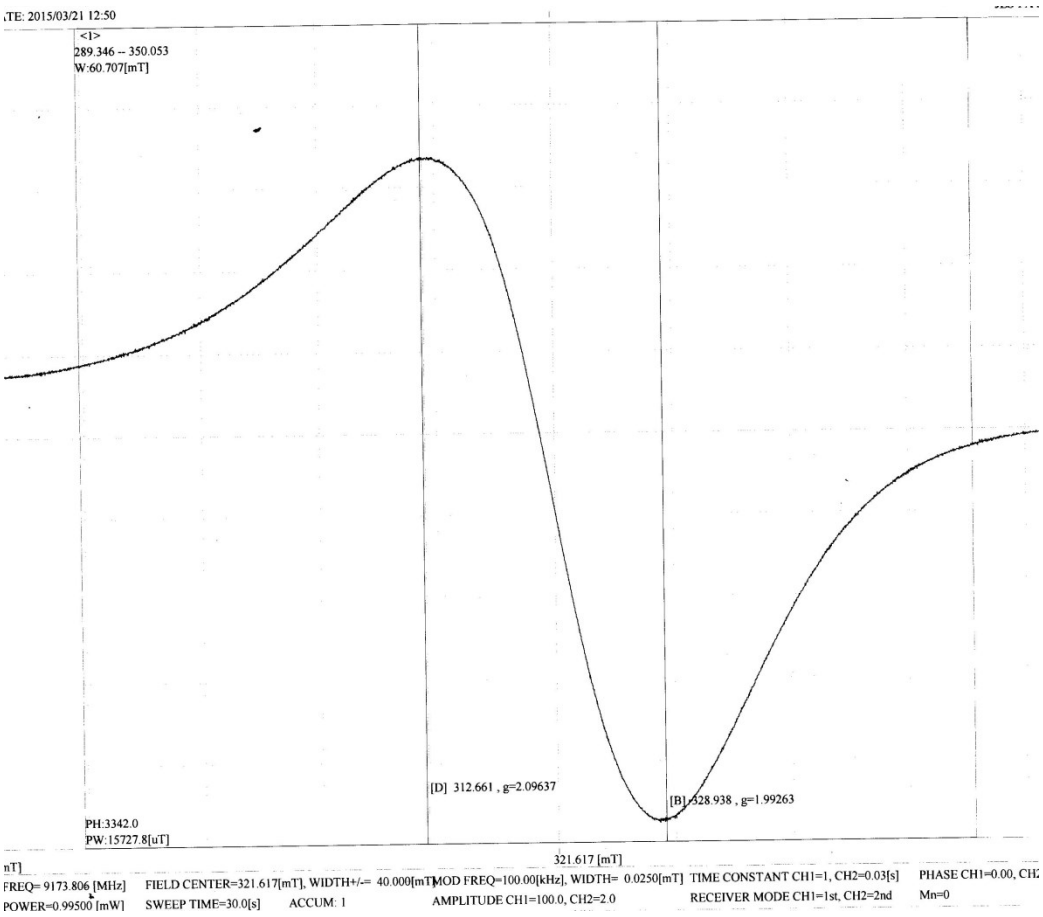

Fig. S3(ii) X–band EPR spectrum of complex 1**b** at RT.

***In vitro* binding studies with ct-DNA**

The comparative spectra of solutions of complexes **1a** and **1b**, in the absence and presence of increasing concentrations of ct-DNA, were measured to obtain evidence for a probable binding mode. As shown in Fig. S4, following addition of increasing aliquots of ct–DNA (0.00-0.5 × 10^{-4} M) to a fixed concentration of complexes **1a** and **1b** (0.2×10^{-4} M), a 'hypochromic effect' was observed in the intra ligand band at 270 nm with a hypsochromic (blue) shift of 2 nm indicating that both complexes interacted with ct-DNA through intercalation mode of binding. The observed hypsochromic shift could be attributed to interaction of a π* orbital of the intercalating ligand (1,10-phen) with a π orbital of the nucleic acid base pair. The differences in binding of L- and D-enantiomers revealed complex **1a** i.e. L-enantiomer exhibited better binding affinity than D-enantiomer.

Further, quantification of the binding strength of complexes **1a** and **1b** towards ct–DNA was ascertained by the intrinsic binding constant, K_b values were calculated by using the Wolfe–Shimer equation (**1**)

$$[DNA]/\varepsilon_a-\varepsilon_f = [DNA]/\varepsilon_b-\varepsilon_f + 1/K_b \left| \varepsilon_b-\varepsilon_f \right| \quad (\mathbf{1})$$

Where, [DNA] is ct–DNA concentration, and ε_a, ε_f and ε_b are the apparent (A_{abs}/[Cu(II) complex]), and free and bound complex extinction coefficients, respectively. A plot of [DNA/]/(ε_a–ε_f) *vs*. [DNA] yields a slope of 1/(ε_b–ε_f) and an intercept of 1/[K_b(ε_b–ε_f)], and K_b values are obtained from the ratio of the slope to the intercept. The intrinsic binding constant K_b values for the complexes **1a** and **1b** were found to 2.48(±0.11) x 10^4 and 1.39(±0.08) x 10^4 M^{-1}, respectively.

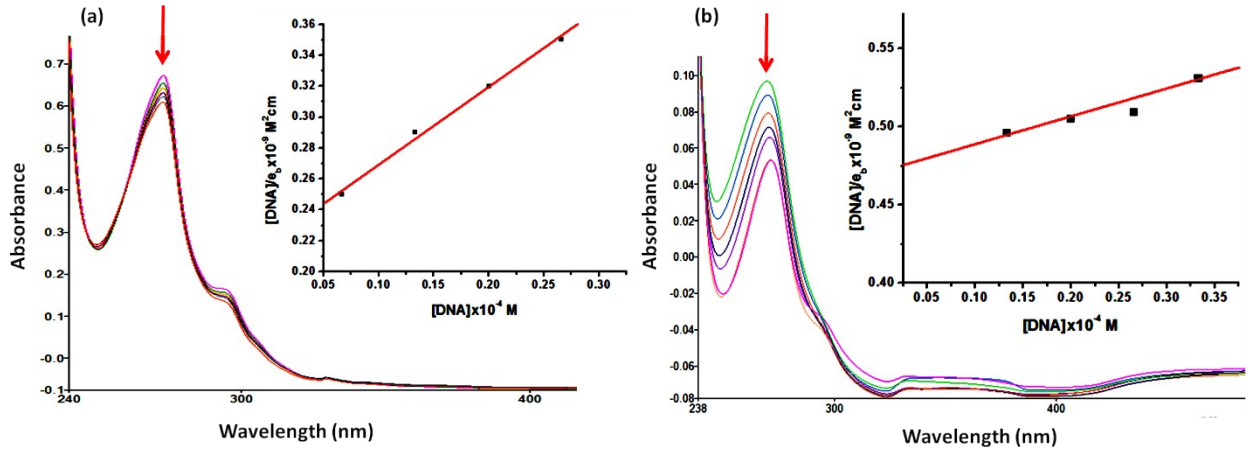

Fig. S4 Absorption spectra of complexes **1a** and **1b** (0.2×10^{-4} M) in the absence and presence of increasing amounts of ct-DNA (0.0–0.5 x 10^{-4} M) in 5.0 mM Tris–HCl buffer at pH 7.2. Inset: Plots of [DNA]/ε_b (M^2 cm) *vs.* [DNA] for titration with complexes **1a** and **1b**.

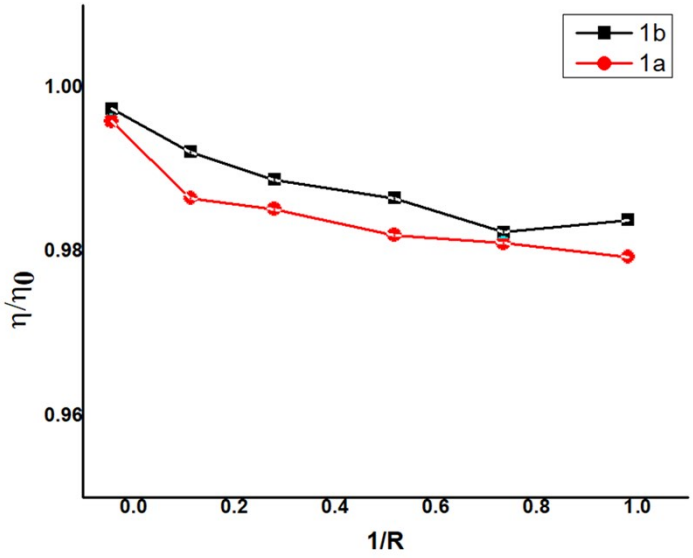

Fig. S5 Effect of increasing amounts of complexes **1a** and **1b** on the relative viscosity (η/η_0) of DNA in Tris–HCl buffer (pH 7.2).

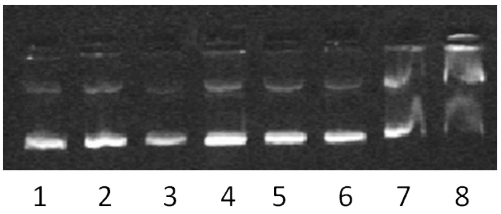

Fig. S6 Cleavage of supercoiled pUC19 DNA (50 μM) by complex **1a** (1 μM) and **1b** (1 μM) in a buffer containing10 mM tris–HCl, pH =7.4 at 37 ºC, for 30 min., Lane (1) DNA starting material; (2) DNA spontaneous reaction 50 μM; (3) asc ; (4) asc + H_2O_2 (5) DNA +

1a; (6) DNA + **1b** (7) DNA+ asc+ H_2O_2+ **1a** (8) DNA+ asc+ H_2O_2+ **1b**; [asc] = 1 mM, [H_2O_2] = 1 mM

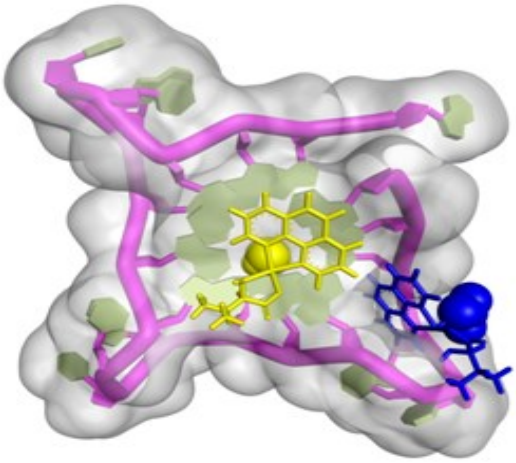

Fig. S7 Top view of the docked pose of complex **1b** with parallel quadruplex G4 structure (PDB ID: 1KF1).